Pattern formation in symplectic coupled map lattices

Leonardo Costa de Souza [a,b] [iD],*, Matheus Rolim Sales [c,d] [iD], José Danilo Szezech Jr. [a,e], Ricardo Luiz Viana [f] [iD], Iberê Luiz Caldas [a], Murilo da Silva Baptista [b] [iD]

[a] *Institute of Physics, University of São Paulo, 05315-970, São Paulo, SP, Brazil*
[b] *Department of Physics, Institute for Complex Systems and Mathematical Biology, SUPA, University of Aberdeen, AB24 3UX, Aberdeen, United Kingdom*
[c] *São Paulo State University (UNESP), Institute of Geosciences and Exact Sciences, 13506-900, Rio Claro, SP, Brazil*
[d] *University of Essex, School of Mathematics, Statistics and Actuarial Science, CO4 3SQ, Wivenhoe Park, Colchester, United Kingdom*
[e] *State University of Ponta Grossa, Department of Mathematics and Statistics, 84030-900, Ponta Grossa, PR, Brazil*
[f] *Federal University of Paraná, Department of Physics, Interdisciplinary Center for Science, Technology and Innovation, Center for Modeling and Scientific Computing, 81531-980, Curitiba, PR, Brazil*

ARTICLE INFO

ABSTRACT

We investigate the emergence of spatio-temporal patterns in a one-dimensional symplectic coupled map lattice (CML) composed of periodically kicked rotors with nonlocal interactions. The system retains the Hamiltonian structure, preserving the phase space volume. The system exhibits cluster states driven by the stickiness effect, where chaotic trajectories wanders around regular structures. By changing the coupling strength and interaction range, we demonstrate the formation of mosaic-like and zigzag patterns associated with transient or persistent clustering. These patterns are analysed using the Kuramoto order parameter, Lyapunov spectrum, and spatial correlation integrals. Our results reveal that pattern formation correlates with suppressed local chaos and small values of Lyapunov exponent, indicating weak chaotic dynamics. The correlation analysis confirms the presence of coherent structures at small scales, which disappear in the strongly chaotic regime. These findings demonstrate how stickiness can induce clustering, given rise to complex collective behaviour in Hamiltonian systems with nonlocal couplings.

1. Introduction

Understanding the emergence of complex spatiotemporal structures in nonlinear systems is a central topic in the study of dynamical systems [1]. One special class is Hamiltonian systems characterized by the symplectic structure of the phase space, they play a fundamental role in modelling conservative physical processes, from celestial mechanics [2,3] to plasma dynamics [4–6]. In the analysis of Hamiltonian systems, the Standard Map is one of the most prominent and paradigmatic systems in nonlinear dynamics, also known as the Chirikov–Taylor map [7,8]. This map describes a kicked rotor with area-preserving dynamics where the phase space is neither entirely regular nor entirely chaotic [9]. The chaotic orbits remain bounded by quasiperiodic curves, which are then limited inside specific domains in phase space [10]. However, even so, the dynamics are far from being obvious, possessing dynamical traps [11] and anomalous diffusion [12]. They arise from subtle, long-term interactions between chaotic and regular regions in phase space that cannot be easily predicted from the systems equations. The earlier cases are described by two-dimensional area-preserving maps, where the islands and the chaotic sea are distinct, disconnected domains.

A crucial question is understanding how trajectories might behave in higher dimensions and whether dynamical traps exist [13]. One way to explore this is through network dynamical systems, like coupled map lattices (CMLs) [14]. They provide a powerful framework to study high-dimensional, discrete-time systems with spatial structure. When constructed with symplectic properties, CMLs preserve key features of Hamiltonian dynamics while allowing exploration of phenomena such as chaotic diffusion [15], and dynamical clustering [16,17]. In dissipative coupled map lattice or networks full synchronization is possible and often expected. The network has the ability to exhibit new features such as chaotic synchronization [18], suppression [19,20], pattern formation [21], multistability [22], and chimera states [23,24]. In Hamiltonian systems, the preservation of phase space volume prevents orbits from collapsing onto an invariant manifold. Synchronization in such systems can be understood as measure synchronization [25], where the trajectories of individual elements explore the same region of phase space similar to the clustering effect [16].

The clustering effect in symplectic CMLs typically manifests as transient [17], where a group of sites shares similar dynamical trajectories. This is a direct consequence of the stickiness effect, that is, the tendency of chaotic trajectories to remain near remnants of regular structures in phase space, in a hierarchical structure of islands around islands [26,27], for finite times. The stickiness effect can happen in different sites at the same time, leading to a cluster [28]. Moreover, the stickiness leads to a confined local chaos, with a multimodal distribution of finite-time Lyapunov exponents [29,30].

In this work, we investigate pattern formation in a one-dimensional symplectic coupled map lattice composed of periodically kicked rotors with nonlocal coupling. By varying the coupling strength and range, we analyse how nonlocal interactions and nonlinear dynamics give rise to distinct spatiotemporal structures, in symplectic systems. We employ dynamical indicators such as the Kuramoto order parameter to quantify the clustering effect, the Lyapunov spectrum, and the spatial correlation integral to characterize the system's behaviour. The key contributions of our study are: the emergence of spatiotemporal collective behaviour characterized by mosaic-like and zigzag structures in the lattice dynamics. This behaviour arises as a consequence of a clustering effect, which collapses orbits into the same region of phase space and leads to long weakly chaotic transients as a direct result.

The present paper is organized as follows: in Section 2, we introduce the coupled map lattice model and their respective limit cases. Section 3 shows the spatio-temporal and cluster effect for the lattice and their parameter dependence. The Lyapunov spectrum for this model are shown in Section 4. Section 5 presents an analysis of the correlation of the spatial component of our model. The last section contains our conclusions.

2. Hamiltonian model and methodology

We consider a system composed of N rotors coupled in a regular one dimension periodic lattice, in the shape of a ring. This systems is described by the Hamiltonian [31,32],

$$H(\mathbf{x}, \mathbf{p}, t) = \sum_{i=1}^{N} \frac{p^{(i)^2}}{2I} + V(\mathbf{x}) \sum_{n=0}^{\infty} \delta(t - n\tau), \tag{1}$$

where $x^{(i)}$ is the angular position of each rotors and $p^{(i)}$ the momentum associated, the potential is given by

$$V(\mathbf{x}) = -\frac{K}{(2\pi)^2 \sqrt{\eta(\alpha)}} \sum_{l=1}^{N} \sum_{j=1}^{N'} \left[\cos\left[2\pi(x^{(l)} - x^{(l+j)})\right] + \cos\left[2\pi(x^{(l)} - x^{(l-j)})\right] \right] \frac{1}{j^\alpha}, \tag{2}$$

where K plays a double role as the non-linearity parameter and the coupling strength. For $K = 0$ the system is uncoupled and integrable. Moreover, we have N as odd and we define $N' = (N - 1)/2$. The coupling is nonlocal given that the summation run over all the neighbours of a given site, but the intensity of the coupling decays with the lattice distance as a power-law, where α represent the range of the coupling and $\eta(\alpha)$ is the normalization factor, this allow us to go from the limit of local coupling, closest neighbours when $\alpha \to \infty$ and global coupling, Hamiltonian mean field [15] when $\alpha \to 0$, let

$$\eta(\alpha) = 2 \sum_{j=1}^{N'} \frac{1}{j^\alpha}, \tag{3}$$

with limit cases as

$$\eta(\alpha) = \begin{cases} N - 1, & \text{in the limit } \alpha \to 0; \\ 2, & \text{in the limit } \alpha \to \infty. \end{cases} \tag{4}$$

The equations of motion is given by the Hamilton equations [33]

$$\frac{dp^{(i)}}{dt} = -\frac{\partial H}{\partial x^{(i)}},$$
$$\frac{dx^{(i)}}{dt} = \frac{\partial H}{\partial p^{(i)}},$$

so that

$$\frac{dp^{(i)}}{dt} = \frac{K}{2\pi \sqrt{\eta(\alpha)}} \sum_{j=1}^{N} \left[\sin\left[2\pi(x^{(i+j)} - x^{(i)})\right] + \sin\left[2\pi(x^{(i-j)} - x^{(i)})\right] \right] \frac{1}{j^\alpha} \sum_{n=0}^{\infty} \delta(t - n\tau),$$
$$\frac{dx^{(i)}}{dt} = \frac{p^i}{I}.$$

The variables $p^{(i)}$ are constant between two impulses, but vary in a discontinuous manner in the impulse. It is possible to obtain a map, integrating the equations of motion around one impulse, with this we arrive in a bi-dimensional map for each site in the network

$$p_{n+1}^{(i)} = p_n^{(i)} + f^{(i)}(\mathbf{x}), \tag{5}$$

$$x_{n+1}^{(i)} = x_n^{(i)} + p_{n+1}^{i} \quad (\text{mod } 1), \tag{6}$$

where

$$f^{(i)}(\mathbf{x}) = \frac{K}{2\pi\sqrt{\eta(\alpha)}} \sum_{j=1}^{N} \left[\sin\left[2\pi(x^{(i+j)} - x^{(i)})\right] + \sin\left[2\pi(x^{(i-j)} - x^{(i)})\right] \right] \frac{1}{j^{\alpha}}. \tag{7}$$

This represents a symplectic coupled map lattice (CML), given that the determinant of the Jacobian matrix is 1, the time and space variables are discrete, allowing us to study the long time behaviour without much computational cost. The total momentum is conserved, thus the motion is bounded to a surface of dimension $2N - 1$. Given the Hamiltonian character of the systems, complete synchronization is impossible. However, clusterization is observed, where the rotors possess the same angular position in the phase space. More precisely, in a cluster with M maps, we have

$$|x_n^{(i)} - x_n^{(j)}| < C, \tag{8}$$

where $i, j = 1, 2, \ldots M$ and $C \ll |x_n^{(i)}|$ is a tolerance level. For the characterization of the degree of clustering, we used, the global R order parameter of Kuramoto [34]. Defined as

$$R(n) = \left| \frac{1}{N} \sum_{j=1}^{N} \exp(2\pi i x_n^{(j)}) \right|. \tag{9}$$

The order parameter R takes values between $[0, 1]$, where $R = 1$ characterize a complete synchronization, and $R = 0$ characterize a complete lack of coherence between the sites. Synchronization appears if the initial conditions are the same for all sites. However, a typical set of initial conditions will most likely not belong to this particular set. In CML high values of R, *i.e.*, values close to 1 help us identify the emergence of cluster effect in the lattice. Studying a model equivalent to ours in the case of global coupling $\alpha = 0$, Konishi and Kaneko [17] have found cluster states occurs when $K < 1$ and the initial conditions are chosen in small intervals, so that, we choose p_0^i as a random distribution in $[-0.05, 0.05]$, with zero sum and x_0^i as a random uniform distribution in the interval $[0.4, 0.6]$, in all further simulations.

3. Cluster effect

Given the high dimensionality of the system it is impossible to see the whole phase space, instead, we choose to show a projection, in Fig. 1, of five randomly selected conjugate pairs $(x^{(i)}, p^{(i)})$ for different values of K, with $\alpha = 5$, on a lattice of 1001 sites. The corresponding time evolution of the order parameter R is also presented. In case (a), the orbits are confined to a small interval in the momentums variable, and the order parameter fluctuates around 0.1, indicating that there is no cluster. In cases (b) and (c), the orbits at all sites remain confined within a small region of phase space, as case (a), but the order parameter is able to detect an apparent coherent motion. The order parameter exhibits regularly spaced peaks, indicating a periodic coherent motion of the lattice sites. Case (d) is similar to (b) and (c), but displays a partial breakdown of the cluster around $n = 0.8 \times 10^4$. In case (e), a similar breakdown occurs, but much earlier in the time evolution, the coherence of the sites are only a transient motion in this case, after with the orbits subsequently spreading over a wider momentum range.

In Fig. 2, we show the time evolution of the position of each site in the lattice. The values of K correspond to the same used in Fig. 1, allowing for a better understanding of the clustering behaviour observed. Pattern formation emerges across the lattice and evolves over time, often taking the form of a zigzag structure, as seen in Figs. 2(b) and (c), which corresponds to the multi-peaked evolution of the order parameter. In Fig. 2(a), a mosaic-like pattern is formed, associated with a low-amplitude order parameter and limited momentum dispersion among the sites. As the coupling and nonlinearity parameter K increases, the patterns are destroy, as illustrated in Figs. 2(d) and (e). In these cases, the zigzag pattern appears only as a transient feature, lasting approximately 7000 and 1000 iterations, respectively. After the transient, we have a "random" pattern, with no correlation between sites of the lattice.

To investigate the temporal coherence of the system across different coupling strengths, we analysed the power spectrum of the Kuramoto order parameter R(n), show in Fig. 1. At the zigzag regime $K = 0.25$ and $K = 0.5$, the spectrum displays a sharp dominant peak along with harmonics, indicating strong periodicity and global spatiotemporal coherence. In contrast, for weak coupling $K = 0.05$ the mosaic-like case, the spectrum is broadband and lacks any dominant frequency. For strong coupling $K = 0.75$ and $K = 1.0$, a initial transient is visible in the time series, but the power spectrum remains largely featureless, with small peaks for the $K = 0.75$ case, suggesting the system enters a chaotic state. These results highlight that the zigzag regime represents a distinct dynamical phase with regular temporal organization, whereas higher coupling strengths lead to a loss of coherent structure.

In order to investigate the dependence of the CML with the parameters bifurcations diagrams can be use [35], however this approach is not directly applicable to our Hamiltonian system. Due to the conservative, symplectic nature of our lattice, there are no attractors and the system does not converge to a steady-state. Instead, it exhibits long-lived transients, stickiness, and persistent fluctuations. Thus to described the gross dynamical nature of the system with the coupling and nonlinearity parameter K and the
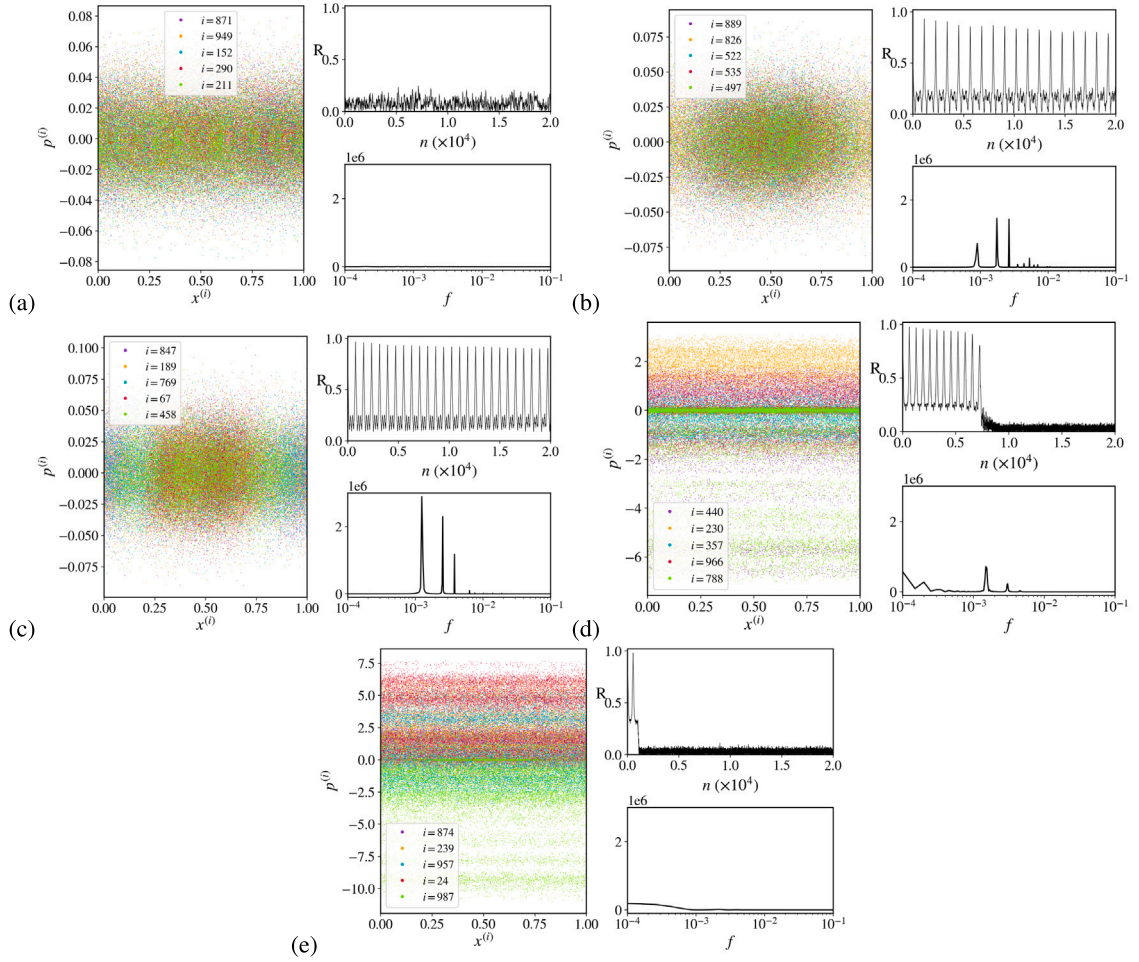
Fig. 1. In the left panel the projection of the phase space, and in the top right panel the time evolution of the order parameter Eq. (9), where in the low right panel, we the power spectrum of the order parameter. For different values of K, in (a) $K = 0.05$, (b) $K = 0.25$, (c) $K = 0.5$, (d) $K = 0.75$ and (e) $K = 1.0$.

coupling range α, we plot the time evolution of the order parameter for different values of K and α. In Fig. 3(a), we fixed $\alpha = 5$ and analysed different values of K. For small $K < 0.2$, the order parameter is close to zero, with scattered points showing higher values, indicating the intermittent formation of a mosaic-like pattern. With the increase of K a structure of stripes appears in the range $0.22 < K < 0.73$, the zigzag pattern is possible. For $K \geq 0.75$ the stripes exists only up to a time, after the order parameter is zero, indicating a transition from the zigzag pattern to the random, unstructured state.

The dependence of the patterns with the coupling range α is showed in Fig. 3(b), where $K = 0.5$. In the case of $\alpha = 0$ the lattice is not clustered corresponding to the unstructured case, the increase of α leads to a cluster with all the sites, the order parameter R is close to one. The further increase of α leads to a transition from full clustering to a transition phase with stripes in the order parameter with different periodicity. For $\alpha > 5$ the lattice converges to the most close neighbour coupling, and we have a structure of stripes where the cluster happens, indicating the establishment of the zigzag pattern in the lattice. The transition from zigzag to chaos is rapid but continuous, as evidenced by the time scales associated with changes in the order parameter. The system evolves from a well-defined zigzag pattern to a mosaic-like structure, and eventually to spatiotemporal chaos.

4. Lyapunov exponents spectrum

The dynamics of the system can be more accurately described through Lyapunov exponents. Even in a network of high dimensions, a positive Lyapunov exponent is a signature that the system is chaotic, while a value of zero corresponds to quasiperiodic motion. The stickiness effect alters dynamical quantifiers such as the Lyapunov exponent, causing its value to be smaller than in the fully chaotic case [29]. In our lattice the Lyapunov spectrum comprises $2N$ exponents, corresponding to each independent eigendirection in the tangent space. Because the system is Hamiltonian, it satisfies
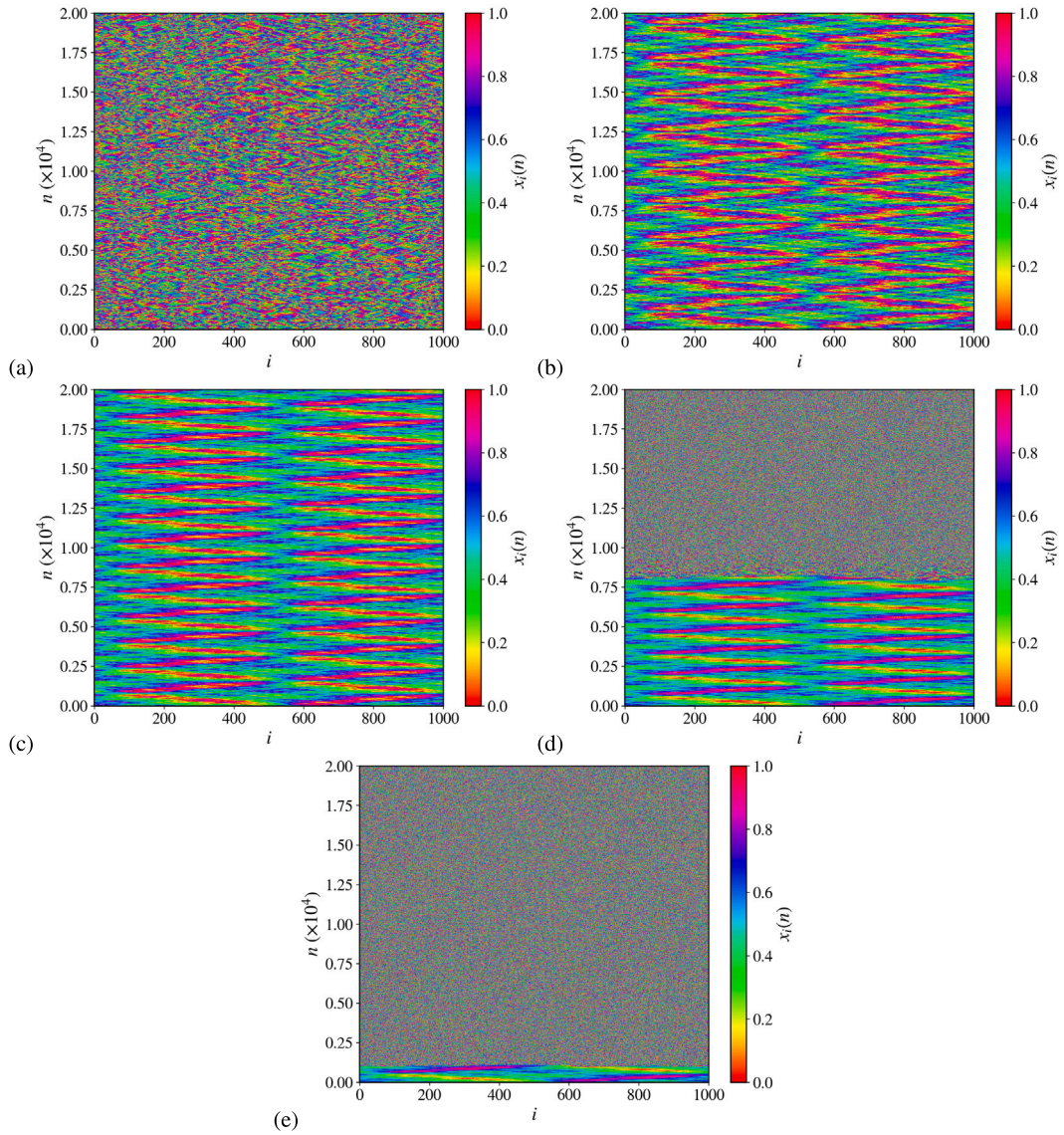
$$\sum_i^{2N} \lambda_i = 0, \tag{10}$$

Fig. 2. In the *y*-axis is time while in the *x*-axis is the site of the lattice and the colours correspond to the position in the left panel and in the right is the momentum. In (a) $K = 0.05$, (b) $K = 0.25$, (c) $K = 0.5$ and (d) $K = 0.75$ and (e) $K = 1.0$.
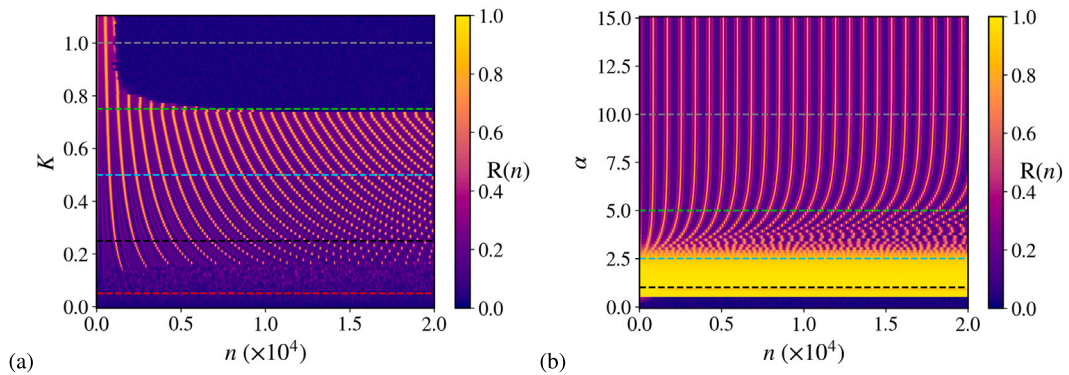

Fig. 3. Time evolution of the order parameter (in colour) as a function of (a) K and (b) α. The horizontal lines in (a) correspond to the same parameters use in Fig. 2.

the exponents cancel in pairs $\lambda_i + \lambda_{i+N} = 0$. This cancellation results in a symmetric spectrum. Furthermore, due to the conservation of momentum, at least one exponent is zero; by symmetry, this means that there are actually two zero exponents. The spectrum can be computed using the method described by Eckmann and Ruelle [36],

$$\lambda_j = \lim_{n \to \infty} \frac{1}{n} \ln \Lambda_j, \tag{11}$$

where is the eigenvalue of the matrix $\mathsf{M} = \prod_{i=0}^{n} \mathcal{J}_n$, we apply a QR decomposition in $\mathcal{J}$, so that, M can be write as a upper triangular matrix, and the eigenvalues are equal to the diagonal elements of this matrix. The Jacobian matrix of the symplectic CML are given by

$$\mathcal{J}_n = \begin{bmatrix} \delta_{i,k} & \frac{\partial f^{(i)}}{\partial x_n^{(k)}} \\ \delta_{i,k} & \delta_{i,k} + \frac{\partial f^{(i)}}{\partial x_n^{(k)}} \end{bmatrix}, \tag{12}$$

where

$$\frac{\partial f^{(i)}}{\partial x_n^{(k)}} = \frac{K}{\sqrt{\eta}} \sum_{j=1}^{N'} \frac{1}{j^\alpha} \left[\cos \left(2\pi (x_n^{(i+j)} - x_n^{(i)}) \right) (\delta_{i+j,k} - \delta_{i,k}) + \cos \left(2\pi (x_n^{(i-j)} - x_n^{(i)}) \right) (\delta_{i-j,k} - \delta_{i,k}) \right]. \tag{13}$$

In Fig. 4, we plot the positive Lyapunov exponents, given the symmetry of the spectrum computed with 2×10^4 iterations. Each curve in Fig. 4(a) corresponds to a specific value of K, as indicated by the vertical lines in Fig. 3(a). The more ordered cluster states, with zigzag pattern $K = 0.25$ and $K = 0.5$ exhibit lower Lyapunov exponents values when compared to the random state observed for $K = 1.0$ and the case where the pattern is lost after some time $K = 0.75$. Moreover, the zigzag patterns possess a smaller Lyapunov exponent spectrum that the mosaic-like pattern $K = 0.05$. In Fig. 4(b), we show the convergence of the maximum Lyapunov exponent, λ_{max}, on a logarithmic scale. The case of $K = 0.75$ exhibits a particularly curious behaviour: the pattern appears to break down at approximately 0.8×10^4 iterations, although a sharp increase in λ_{max} is already observed around 0.5×10^4 iterations, thus, the Lyapunov exponent serve as an early indicator of the behaviour transition in the CML.

Fig. 4(c) present the positive Lyapunov spectrum for $K = 0.5$ and five values of α corresponding to the vertical lines in Fig. 1(b). In Fig. 4(d) the convergence of the maximum Lyapunov exponent is presented. The case without clustering exhibits higher Lyapunov exponent values, while the cases with clustering display a small Lyapunov spectrum with also exponents of the order of 10^{-3}, indicating that certain degrees of motion are not fully chaotic. The case without clustering exhibits higher Lyapunov exponent values, while the cases with clustering display a small Lyapunov spectrum with also exponents of the order of 10^{-3}. Moreover, Szezech et al. [29] showed that the finite-time Lyapunov exponent (FTLE) exhibits a bimodal distribution in the Standard Map, reflecting the intermittent behaviour of orbits as they alternate between trapping regions and the chaotic sea. This result suggests that the small values Lyapunov exponents detected in the presence of emergent patterns are a consequence of the stickiness effect, which alters the dynamical properties of the orbits. Stickiness, therefore, can be understood as the underlying mechanism driving the formation of clusters, as discussed in [16,28], and these clusters, in turn, give rise to spatiotemporal patterns. Unlike the typical intermittent stickiness seen in low-dimensional Hamiltonian systems, in our coupled map lattice, this effect can be persistent, as observed in Figs. 1(a)–(c), or transient, as in Figs. 1(d) and (e).

5. Spatial correlation integral

Another important measure for the clustering effect is the correlation integral [37,38] $C_n(\ell)$, it is a fundamental tool in nonlinear dynamics used to quantify the spatial and temporal structure of trajectories in phase space. By measuring the probability that two points from a trajectory are within a given distance ℓ of each other, the correlation integral captures how densely points cluster over time. The correlation integral is defined as

$$C_n(\ell) = \lim_{n \to \infty} \frac{1}{N^2} \sum_{\substack{i,j=1 \\ i \neq j}}^{N} \Theta(\ell - \|x^{(i)} - x^{(j)}\|), \tag{14}$$

where Θ is the Heaviside step function, $\| \dots \|$ is a distance, in our case the Euclidean metric, and ℓ is the correlation radius. If $C_n(\ell)$ increases quickly with ℓ the system exhibits strong spatial correlation, while if the remains low or increases slowly, the system is spatially uncorrelated (randomly distributed states). Moreover, a high value of $C_n(\ell)$ for small ℓ indicates that the system is in a cluster and we have a strong collective behaviour [37,38].

In Fig. 5 we showed the time evolution of the correlation integral as a function of ℓ for a fixed value of $\alpha = 5$ and different values of K. A sharp transition is observed around $\ell = 0.7$ for the mosaic-like case Fig. 5(a), while the zigzag and random cases this transition happens around $\ell = 0.5$, after this correlation abruptly saturates to 1, indicating that most point pairs fall within this distance in phase space. Below this threshold, the presence of horizontal stripe patterns, Figs. 5(b), (c) and (d) reveals temporal regularities in the lattice evolution, up to some time. The horizontal stripes repeat almost identically from one driving period to the next, indicating that the lattice enters a nearly periodic pattern in time. In other words, the same spatial pattern recurs each kick, so the dynamics appears locked in time.

Grassberger and Procaccia [37] introduce the calculation of the correlation integral as a way to estimate the dimension of correlation γ, using the fact that if the number of points use to calculate C_n is sufficiently large, then $C_n(\ell) \sim \ell^\gamma$. Thus a log–log
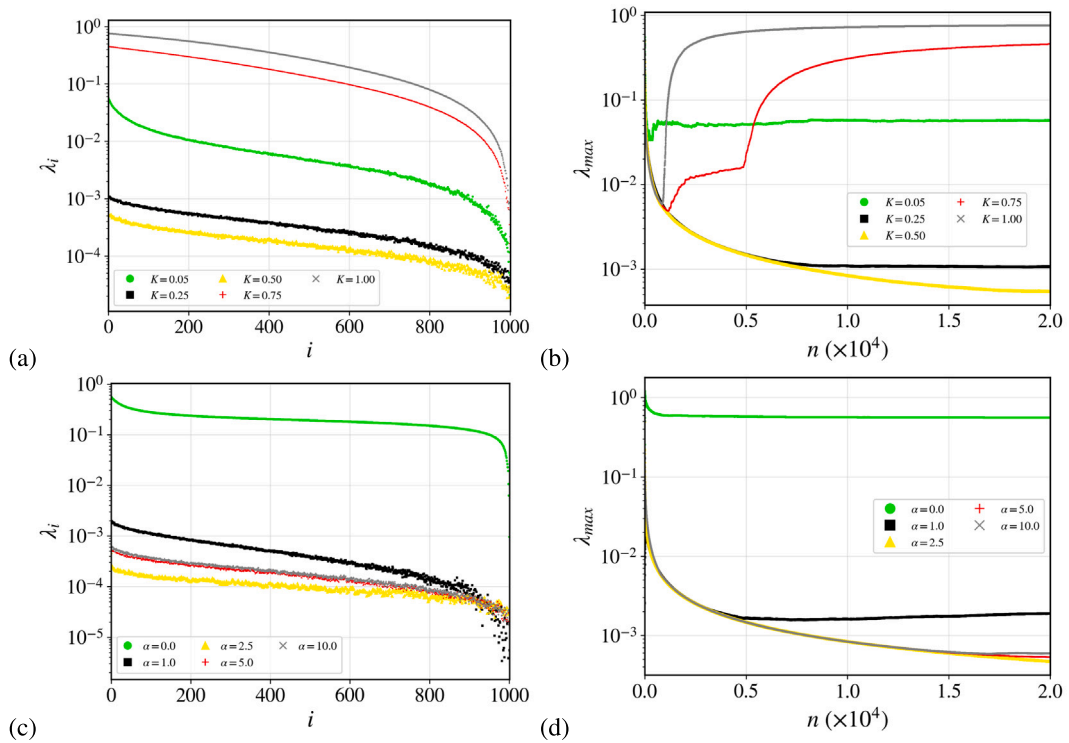
Fig. 4. In (a) Positive Lyapunov exponents for different values of K and $\alpha = 5.0$. In (b) convergence of the maximum Lyapunov exponent for $K = 0.5$ and $\alpha = 5.0$. In (c) Positive Lyapunov exponents for different values of α and $K = 0.5$. In (d) convergence of the maximum Lyapunov exponent for $K = 0.5$ and different values of α.

plot of the correlation integral versus ℓ gives a estimate of γ. This dimension measures the occupation of the phase space. If $\gamma \sim 0$ the points are very close in the phase space, thus cluster motion, while $\gamma = 1$ the orbits are far apart. Given the finite time of our simulations the correlation integral is the actually the correlation sum, and is computed considering the trajectories in time n of all sites. In Fig. 6 we show the time evolution of the correlation dimension for the coupled map lattice with $n = 1001$, $\alpha = 5$ and $K = 0.75$, the dimension presents a cyclic behaviour when the zigzag pattern exist oscillating between 0 and 0.9 until the transition to chaos when the dimension to the unit, meaning not that the points are far apart without correlation.

These results suggest that the orbits in this case are confined to simple invariant structures rather that the full phase space. These invariant structures are most probably the stable periodic orbits of low dimension that persist for large perturbation until the onset of chaos as observe in other Hamiltonian lattices [39,40] like in the Fermi Pasta Ulam problem [41,42]. The stickiness effect occurs around these low dimension orbits leading to clustering in a region of the phase space. Thereafter, we have a weakly chaotic behaviour. This structured pattern implies that, despite the nonlinearity of the underlying dynamics, the system does not exhibit fully developed chaos and retains a degree of spatiotemporal organization. A further increase in coupling strength, which leads to the breakdown of spatial patterns, also results in a loss of correlation between sites. This is evident in Figs. 5(d) and (e). This suggests that the system has entered a more chaotic regime, with trajectories rapidly mixing in phase space and losing coherent temporal structures. The correlation saturates more uniformly as ℓ increases, indicating that most point pairs become quickly uncorrelated at small scales and fully correlated at larger scales. Exists a small transient dynamics in the case of $K = 1.0$, but overall the behaviour reflects a dominant chaotic regime.

It is also possible to define average time spatial correlation $n\ C_s$ as,

$$C_s(\ell) = \langle (x_n^{(i)} - \bar{x}_n)(x_n^{(i+\ell)} - \bar{x}_n) \rangle_{i,n}, \tag{15}$$

where $\bar{x}_n$ is the spatial average at the time n, this is the two point correlation function it measures how the value at one site influences or correlates with sites at a distance ℓ. In Fig. 7, we showed the spatial correlation as a function of the lattice distance. For the case the zigzag pattern Fig. 7(a) we have a high correlation for small distances, sites close to each other are strong correlated, as the distance increases the correlations decays quickly to zero. The best fit determined by the small root mean square error, was found to be a stretched exponential of the form $\exp(-(\ell/\gamma)^\beta)$, where $\beta = 0.91$ is the stretching exponent and $\gamma = 28.68$ the correlation length. Thus, sites $\ell < 30$ are strongly correlated, while for $\ell \gg 30$ they have a weak correlation. The stretching parameter β indicates that the decay is slower that a pure exponential, long range correlations are still present but they are weaker at large distances. Fig. 7(b) shows the spatial correlation with the distance, where the fitted curve an exponential of the form $\exp -(\ell/105.06)$. The correlations are small, around 0.02 for neighbour sites and goes to zero with the increase of the distance.
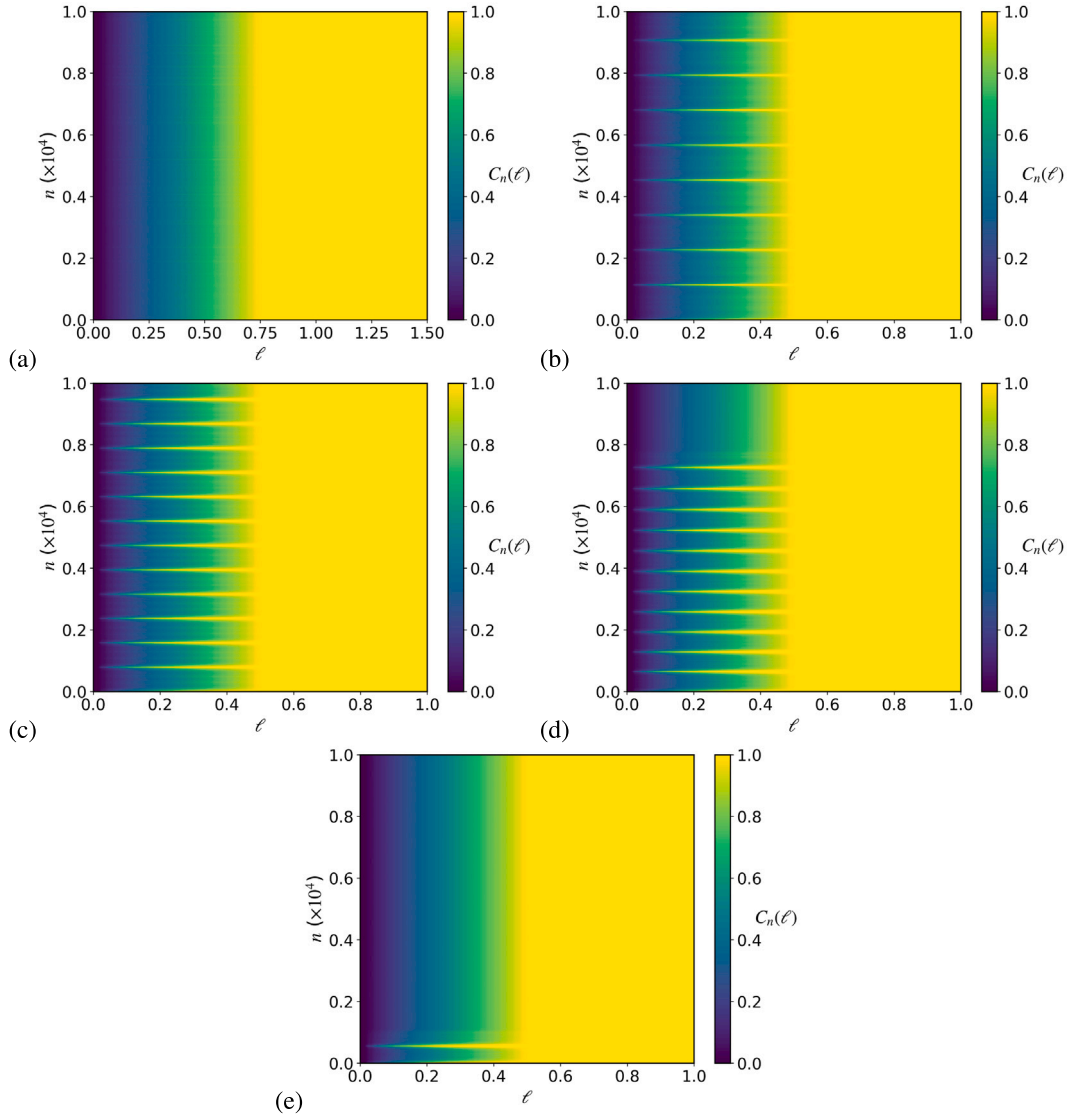
Fig. 5. Time evolution of the correlation integral, as colour, for different values of the correlation radius ℓ. In (a) $K = 0.05$, (b) $K = 0.25$, (c) $K = 0.5$, (d) $K = 0.75$, (e) $K = 1.0$ and $\alpha = 5$ in all cases.

6. Conclusions

In this work, we explored the emergence of spatiotemporal patterns in a one-dimensional symplectic coupled map lattice composed of periodically kicked rotors with nonlocal interactions. Due to the symplectic structure of the system, the orbits do not collapse onto an invariant manifold, making full synchronization possible only for a special set of initial conditions. To typical initial conditions, we observe the formation of cluster states, which emerge as a consequence of the stickiness effect, where chaotic trajectories become temporarily confined near regular structures in phase space, causing the orbits to group together.

Our findings reveal the existence of mosaic-like patterns $K = 0.025$ and zigzag structures $K = 0.5$ for different values of coupling strength and coupling range. In these configurations, the Lyapunov exponent spectrum exhibits significantly smaller values compared to the case without correlations or spatial patterns between sites. Lyapunov exponents very close to zero on the order of 10^{-4} are also observed, indicating that the motion is restricted to certain degrees of freedom rather than spanning the entire available phase space. The Lyapunov exponents alone cannot precisely determine the dimension of these regions. However, this limitation could be overcome using the Generalized Alignment Index (GALI) [43–45]. For an s-dimensional torus, GALI$_k$ remains nearly constant for $k \leq s$ and decays algebraically for $k > s$, whereas for a chaotic orbit, all GALI$_k$ decay exponentially [45]. Thus, measuring the GALIs would directly reveal whether a trajectory lies on a low-dimensional torus (stable mode) and determine its dimension.
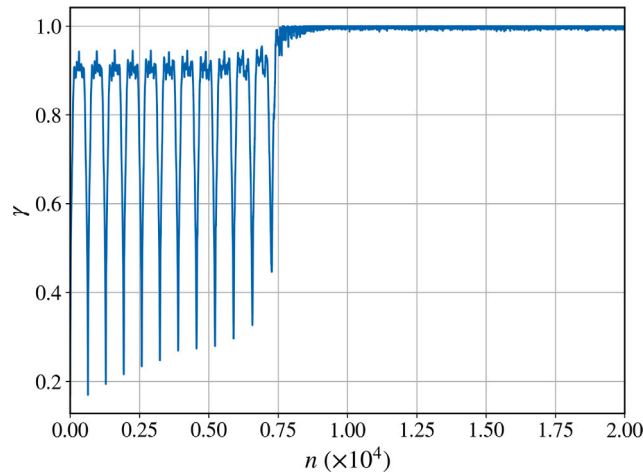
Fig. 6. Time evolution of the correlation dimension estimate from the log–log plot of $C_n(\ell) \times \ell$, for $\alpha = 5$ and $K = 0.75$.
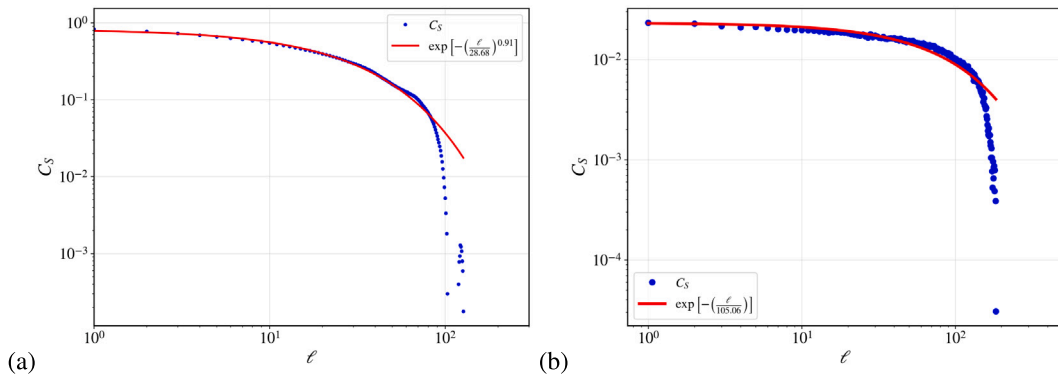

Fig. 7. In (a) and (b) is presented the decay of the average time spatial correlation, for the parameter of $K = 0.50$ zigzag and $k = 1.00$ chaos, respectively.

The analysis of the order parameter is complemented by the correlation integral, which is capable of revealing collective behaviour in the lattice. For mosaic-like and zigzag patterns, strong correlations are observed even at small correlation radii, appearing in a periodic fashion, similar to the order parameter. In contrast, for high coupling strength and nonlinearity K, correlation appears in a transient time, and significant correlations only emerge at large correlation radii, indicating a lack of clusterization or coherence between sites in the lattice. The spatial correlations decays as a stretched exponential for zig-zag pattern and as a exponential curve for the fully chaotic case, however in the last case the correlations are very small.

The emergence of spatial patterns in the lattice is closely linked to the phenomenon of clusterization, where the orbits of different sites evolve in coherent manner. Our results indicate that this behaviour is associated with a regime of weak chaos, as evidenced by small but positive Lyapunov exponents. During this phase, the system explores a restricted region of phase space, as show by the correlation dimension, suggesting that trajectories become temporarily confined, this is consistent with the phenomenon of stickiness observed in Hamiltonian dynamics. This dynamical trapping leads to long coherence and spatial ordering that depends on the strength and range of the coupling with some cases showing a transition to more chaotic state or only a chaotic state. Therefore, our findings support the interpretation that cluster formation arises as a manifestation of stickiness in symplectic systems with nonlocal interactions. Open questions remain regarding how clustering correlates with intermittent stickiness synchronization, as discussed in [28], as well as how energy and information is transported between the sites of the lattice.

CRediT authorship contribution statement

Leonardo Costa de Souza: Writing – review & editing, Writing – original draft, Visualization, Software, Methodology, Investigation, Formal analysis, Data curation, Conceptualization. **Matheus Rolim Sales:** Writing – review & editing, Software, Investigation, Formal analysis, Data curation. **José Danilo Szezech:** Writing – review & editing, Writing – original draft, Supervision, Project administration, Formal analysis. **Ricardo Luiz Viana:** Writing – review & editing, Supervision, Methodology, Conceptualization. **Iberê Luiz Caldas:** Writing – review & editing, Supervision, Project administration, Methodology, Funding acquisition, Conceptualization. **Murilo da Silva Baptista:** Writing – review & editing, Supervision, Investigation.

Declaration of competing interest

The authors declare that they have no known competing financial interests or personal relationships that could have appeared to influence the work reported in this article.

Acknowledgements

Data availability

Data will be made available on request.

References

[1] Strelkova GI, Anishchenko VS. Spatio-temporal structures in ensembles of coupled chaotic systems. Phys-Usp 2020;63(2):145.

[2] Koon WS, Lo MW, Marsden JE, Ross SD. Dynamical systems, the three-body problem and space mission design. Springer New York; 2017.

[3] Tremaire S. Dynamics of planetary systems. Princeton University Press; 2023.

[4] Morrison PJ. Hamiltonian and action principle formulations of plasma physics. Phys Plasmas 2005;12(5):10.

[5] Escande DF. From thermonuclear fusion to Hamiltonian chaos. Eur Phys J H 2018;43:397–420.

[6] Viana RL, Mugnaine M, Caldas IL. Hamiltonian description for magnetic field lines in fusion plasmas: A tutorial. Phys Plasmas 2023;30(9).

[7] Chirikov BV. Research concerning the theory of non-linear resonance and stochasticity. Geneva: CERN; 1971, Translated at CERN from the Russian (IYAF-267-TRANS-E). URL https://cds.cern.ch/record/325497.

[8] Chirikov BV. A universal instability of many-dimensional oscillator systems. Phys Rep 1979;52(5):263–379. http://dx.doi.org/10.1016/0370-1573(79)90023-1.

[9] Lichtenberg A, Lieberman M. Regular and chaotic dynamics. In: Applied mathematical sciences, Springer New York; 2013, URL https://books.google.com.br/books?id=pR3aBwAAQBAJ.

[10] Ott E. Chaos in dynamical systems. 2nd ed.. Cambridge University Press; 2002.

[11] Zaslavsky G. Dynamical traps. Phys D: Nonlinear Phenom 2002;168–169:292–304. http://dx.doi.org/10.1016/S0167-2789(02)00516-X, VII Latin American Workshop on Nonlinear Phenomena. URL https://www.sciencedirect.com/science/article/pii/S016727890200516X.

[12] Shlesinger MF, Zaslavsky GM, Klafter J. Strange kinetics. Nature 1993;363(6424):31–7. http://dx.doi.org/10.1038/363031a0.

[13] Falcioni M, Marconi UMB, Vulpiani A. Ergodic properties of high-dimensional symplectic maps. Phys Rev A 1991;44(4):2263.

[14] Chazottes J-R, Fernandez B. In: Dynamics of coupled map lattices and of related spatially extended systems, vol. 671, Springer Science & Business Media; 2005.

[15] Latora V, Rapisarda A, Ruffo S. Superdiffusion and out-of-equilibrium chaotic dynamics with many degrees of freedoms. Phys Rev Lett 1999;83(11):2104.

[16] Woellner CF, Lopes SR, Viana RL, Caldas IL. Clustering and diffusion in a symplectic map lattice with non-local coupling. Chaos Solitons Fractals 2009;41(5):2201–15.

[17] Konishi T, Kaneko K. Clustered motion in symplectic coupled map systems. J Phys A: Math Gen 1992;25(23):6283.

[18] Boccaletti S, Kurths J, Osipov G, Valladares D, Zhou C. The synchronization of chaotic systems. Phys Rep 2002;366(1):1–101. http://dx.doi.org/10.1016/S0370-1573(02)00137-0, URL https://www.sciencedirect.com/science/article/pii/S0370157302001370.

[19] Molgedey L, Schuchhardt J, Schuster H. Suppressing chaos in neural networks by noise. Phys Rev Lett 1992;69(26):3717–9. http://dx.doi.org/10.1103/PhysRevLett.69.3717, Cited by: 106. URL https://www.scopus.com/inward/record.uri?eid=2-s2.0-0000733651&doi=10.1103%2fPhysRevLett.69.3717&partnerID=40&md5=4fc5ae18f1ae705a5a9d0dbf4c1d9adb.

[20] Matías M, Güémez J. Chaos suppression in flows using proportional pulses in the system variables. Phys Rev E - Stat Phys Plasmas, Fluids, Related Interdiscip Top 1996;54(1):198–209. http://dx.doi.org/10.1103/PhysRevE.54.198, Cited by: 23. URL https://www.scopus.com/inward/record.uri?eid=2-s2.0-0000609875&doi=10.1103%2fPhysRevE.54.198&partnerID=40&md5=79b9709697cc181f841c16dfa3fac1dd.

[21] Lind PG, Corte-Real J, Gallas JAC. Pattern formation in diffusive-advective coupled map lattices. Phys Rev E 2004;69:066206. http://dx.doi.org/10.1103/PhysRevE.69.066206, URL https://link.aps.org/doi/10.1103/PhysRevE.69.066206.

[22] de Freitas MST, Viana RL, Grebogi C. Multistability, basin boundary structure, and chaotic behavior in a suspension bridge model. Int J Bifurc Chaos 2004;14(03):927–50. http://dx.doi.org/10.1142/S0218127404009636, arXiv:https://doi.org/10.1142/S0218127404009636.

[23] Abrams D, Strogatz S. Chimera states for coupled oscillators. Physical Review Letters 2004;93(17). http://dx.doi.org/10.1103/PhysRevLett.93.174102.

[24] dos Santos V, Sales MR, Muni SS, Szezech Jr. JD, Batista AM, Yanchuk S, et al. Identification of single- and double-well coherence-incoherence patterns by the binary distance matrix. Communications Nonlinear Science Numerical Simulation 2023;125. http://dx.doi.org/10.1016/j.cnsns.2023.107390.

[25] Hampton A, Zanette DH. Measure synchronization in coupled Hamiltonian systems. Phys Rev Lett 1999;83(11):2179.

[26] Sales MR, Mugnaine M, Szezech J, Viana RL, Caldas IL, Marwan N, et al. Stickiness and recurrence plots: An entropy-based approach. Chaos: An Interdiscip J Nonlinear Sci 2023;33(3):033140. http://dx.doi.org/10.1063/5.0140613, arXiv:https://pubs.aip.org/aip/cha/article-pdf/doi/10.1063/5.0140613/16822537/033140_1_5.0140613.pdf.

[27] Souza L, Sales M, Mugnaine M, Szezech Jr. J, Caldas I, Viana R. Chaotic escape of impurities and sticky orbits in toroidal plasmas. Phys Rev E 2024;109(1):015202.

[28] da Silva RM, Manchein C, Beims MW. Intermittent stickiness synchronization. Phys Rev E 2019;99(5):052208.

[29] Szezech JD, Lopes SR, Viana RL. Finite-time Lyapunov spectrum for chaotic orbits of non-integrable Hamiltonian systems [rapid communication]. Phys Lett A 2005;335(5–6):394–401. http://dx.doi.org/10.1016/j.physleta.2004.12.058.

[30] Harle M, Feudel U. Hierarchy of islands in conservative systems yields multimodal distributions of FTLEs. Chaos Solitons Fractals 2007;31(1):130–7. http://dx.doi.org/10.1016/j.chaos.2005.09.031, URL https://www.sciencedirect.com/science/article/pii/S0960077905008908.

[31] Rogers JL, Wille LT. Phase transitions in nonlinear oscillator chains. Phys Rev E 1996;54:R2193–6. http://dx.doi.org/10.1103/PhysRevE.54.R2193, URL https://link.aps.org/doi/10.1103/PhysRevE.54.R2193.

[32] Woellner C, Lopes S, Viana R, Caldas I. Clustering and diffusion in a symplectic map lattice with non-local coupling. Chaos Solitons Fractals 2009;41(5):2201–15. http://dx.doi.org/10.1016/j.chaos.2008.08.026, URL https://www.sciencedirect.com/science/article/pii/S0960077908003986.

[33] Lichtenberg AJ, Lieberman MA. In: Regular and chaotic dynamics, vol. 38, Springer Science & Business Media; 2013.

[34] Kuramoto Y. Chemical turbulence. Springer Berlin Heidelberg; 1984, p. 111–40.

[35] Sinha S. Random coupling of chaotic maps leads to spatiotemporal synchronization. Phys Rev E 2002;66:016209. http://dx.doi.org/10.1103/PhysRevE.66.016209, URL https://link.aps.org/doi/10.1103/PhysRevE.66.016209.

[36] Eckmann J, Ruelle D. Rev. Mod. Phys.. Rev Modern Phys 1985;57(617).

[37] Grassberger P, Procaccia I. Measuring the strangeness of strange attractors. Phys D: Nonlinear Phenom 1983;9(1–2):189–208.

[38] Vasconcelos D, Viana R, Lopes S, Batista A, de S. Pinto S. Spatial correlations and synchronization in coupled map lattices with long-range interactions. Phys A 2004;343:201–18. http://dx.doi.org/10.1016/j.physa.2004.06.063, URL https://www.sciencedirect.com/science/article/pii/S0378437104008568.

[39] Antonopoulos C, Bountis T. Stability of simple periodic orbits and chaos in a Fermi-Pasta-Ulam lattice. Phys Rev E 2006;73:056206. http://dx.doi.org/10.1103/PhysRevE.73.056206, URL https://link.aps.org/doi/10.1103/PhysRevE.73.056206.

[40] Bountis T. Stability of motion: From Lyapunov to the dynamics of N-degree of freedom Hamiltonian systems.. Nonlinear Phenomena Complex Systems 2006;9(3):209–39.

[41] Fermi E, Pasta P, Ulam S, Tsingou M. Studies of the nonlinear problems. Tech. rep., Los Alamos, NM (United States: Los Alamos National Laboratory (LANL); 1955.

[42] Berman G, Izrailev F. The Fermi–Pasta–Ulam problem: fifty years of progress. Chaos: An Interdiscip J Nonlinear Sci 2005;15(1).

[43] Skokos C, Antonopoulos C, Bountis TC, Vrahatis MN. Smaller alignment index (SALI): Determining the ordered or chaotic nature of orbits in conservative dynamical systems. In: Libration point orbits and applications. World Scientific; 2003, p. 653–64. http://dx.doi.org/10.1142/9789812704849_0030, URL http://www.worldscientific.com/doi/abs/10.1142/9789812704849_0030.

[44] Skokos C, Bountis TC, Antonopoulos C. Geometrical properties of local dynamics in Hamiltonian systems: The generalized alignment index (GALI) method. Phys D: Nonlinear Phenom 2007;231:30–54. http://dx.doi.org/10.1016/j.physd.2007.04.004.

[45] Skokos C, Bountis T, Antonopoulos C. Detecting chaos, determining the dimensions of tori and predicting slow diffusion in Fermi–Pasta–Ulam lattices by the generalized alignment index method. Eur Phys J Spec Top 2008;165(1):5–14.